

Transverse patterns in nascent optical bistability

M. Tlidi, M. Georgiou, and Paul Mandel

Université Libre de Bruxelles, Campus Plaine, Code Postal 231, 1050 Bruxelles, Belgium

(Received 25 May 1993)

We study the Swift-Hohenberg equation describing a passive optical cavity driven by an external coherent field, valid close to the onset of optical bistability. A linear analysis shows that the system can sustain nontrivial stationary structures for small positive detunings. A weakly nonlinear analysis in the vicinity of the instability points reveals the existence of stable hexagonal structures which eventually give way to rolls. Numerical simulations support such a bifurcation scenario.

PACS number(s): 42.65.Pc, 42.60.Mi

I. INTRODUCTION

The emergence of patterns in passive optical systems due to transverse effects has been the subject of recent investigations [1]. More specifically, analytical studies on models of optical bistability have demonstrated that static and dynamic structures may be sustained by these systems whether we impose or relax the mean-field approximation [2–4]. Such analyses, though, have been confined to a single transverse dimension. Two-dimensional patterns associated with the interplay between the longitudinal and transverse dimensions have been reported [5], albeit restricted to numerical results.

Recently, the mean-field model of optical bistability in the dispersive limit derived by Lefever and Lugiato in [2] has been shown to sustain spatial dissipative structures in two dimensions [6]. The numerical simulations reveal the existence of hexagons and exhibit reasonable agreement with the nonlinear analysis in the vicinity of the instability points. This model, though, fails to describe accurately possible stationary patterns close to the transistor characteristic and the onset of optical bistability. The study of such a regime requires a two-time analysis that introduces an additional slow time scale which is of geometrical and not of physical origin, as was pointed out in [7]. Moreover, it was shown there that a global description of the field in terms of a generalized Ginzburg-Landau equation is possible unless the detuning is finite and positive. In this paper, we concentrate on this latter model and we undertake an analytical and numerical study of possible dissipative structures in two transverse dimensions.

II. DESCRIPTION OF THE MODEL

We consider a ring cavity filled with two-level atoms without population inversion, driven by a coherent plane-wave steady beam. Starting from the Maxwell-Bloch equations, the deviation X of the electric field from its value at the onset of bistability is shown to obey the equation [7]

$$\frac{\partial X}{\partial t} = 4(1 + i\Delta)y + X(\mathcal{C} - |X|^2) - 4a\Delta\mathcal{L}_1X - \frac{4}{3}a^2\mathcal{L}_1\mathcal{L}_1X, \quad (2.1)$$

where \mathcal{C} is the deviation of the cooperativity parameter C from $C_{\text{crit}} = 4(1 + \Delta^2)$, and $y = Y - (\sqrt{3}/2)\mathcal{C}$, with Y the deviation of the amplitude of the injected field from $Y_{\text{crit}} = 3\sqrt{3}(1 + \Delta^2)$. C_{crit} and Y_{crit} correspond to the values of C and Y , respectively, at the onset of bistability. $\Delta = (\omega_a - \omega_e)/\gamma_\perp$, where ω_a and ω_e are the atomic and the external frequencies respectively, γ_\perp is the decay rate of the atomic polarization, \mathcal{L}_1 is the transverse Laplacian, and a is proportional to the spacing between two adjacent transverse modes. We have redefined time in terms of a constant that involves the decay rates of the electric field, the polarization, and the population inversion, respectively. Equation (2.1) is valid in the domain $-|O(1/\epsilon)| \leq \Delta \leq |O(\epsilon)|$, where ϵ denotes the distance from the onset of bistability. In the weakly dispersive limit $\Delta \leq |O(\epsilon)|$, it may be reduced to

$$\frac{\partial X}{\partial t} = 4y + X(\mathcal{C} - X^2) - 4a\Delta\mathcal{L}_1X - \frac{4}{3}a^2\mathcal{L}_1\mathcal{L}_1X \quad (2.2)$$

with X real. This is a real Swift-Hohenberg type equation, in contrast to the complex Ginzburg-Landau equation that has already been studied in the context of optical bistability [2]. As will become evident in the next section, retaining the Laplacian term is crucial for the emergence of nontrivial spatial patterns. It is this last equation (2.2) that we concentrate on in this paper.

III. LINEAR AND WEAKLY NONLINEAR ANALYSIS

The homogeneous steady states of Eq. (2.2), satisfy the cubic equation,

$$4y_s = X_s(X_s^2 - \mathcal{C}), \quad (3.1)$$

where the subscript s is used to denote the stationary values of the real functions X and y , respectively. The

steady-state curve X_s , as a function of y_s , is single valued for $\mathcal{C} < 0$ and multivalued for $\mathcal{C} > 0$. Its linear stability is determined by linearizing Eq. (2.2) around it and seeking solutions for the deviation in the form $\exp(\lambda t + i\mathbf{k}\cdot\mathbf{r})$, where \mathbf{r} refers to the transverse coordinates. Assuming the relation $(\mathcal{L}_1 + k^2)\exp(i\mathbf{k}\cdot\mathbf{r}) = 0$, this analysis yields the equation

$$\lambda = \mathcal{C} - 3X_s^2 + 4\Delta ak^2 - \frac{4}{3}a^2k^4 \quad (3.2)$$

for the characteristic real root λ . The condition $\lambda = 0$ leads to a k -dependent neutral stability curve which determines that inhomogeneous spatial patterns may arise spontaneously only if $\Delta > 0$, and at the critical value of X_s

$$X_{s,c}^2 = \Delta^2 + \mathcal{C}/3. \quad (3.3)$$

Thus the neutral stability curve has a minimum at $X = X_{s,c}$. The most unstable modes at the onset of the instability fall on a circle of magnitudes $|k_c|^2 = 3\Delta/2a$. In Fig. 1 we have shown the instability domains for a monostable ($\Delta = 0.1, \mathcal{C} = -0.025$), and a bistable ($\Delta = 0.1, \mathcal{C} = 0.025$) case, respectively. Since Eq. (3.3) is valid for symmetric positive and negative values of X and y , respectively, we conclude that there is always a pair of instability points.

We now treat the nonlinear evolution of the system in the vicinity of the critical points by employing standard bifurcation techniques [8]. Such an analysis allows us to

derive analytically amplitude equations for possible emanating transverse structures and assess their stability. To this end, we introduce in Eq. (2.2) the new variable $u(\mathbf{r}, t)$, defined by

$$X = X_s + u(\mathbf{r}, t) \quad (3.4)$$

with

$$u = \eta(u_0 + \eta u_1 + \eta u_2 + \dots), \quad (3.5)$$

where the small parameter η measures the distance from the bifurcation point. We also expand the bifurcation parameter y and X_s around their critical values $a_0 = X_{s,c}$, and $y_0 = y_{s,c}$, respectively,

$$X_s = a_0 + \eta a_1 + \eta^2 a_2 + \dots, \quad (3.6)$$

$$y = y_0 + \eta y_1 + \eta^2 y_2 + \dots, \quad (3.7)$$

and introduce the slow time $\tau = \eta^2 t$.

The solution to the leading-order homogeneous problem can be approximated as a linear superposition of the critical modes \mathbf{k}_i :

$$u(\mathbf{r}, t) = \sum_{i=1}^m (W_i e^{i\mathbf{k}_i \cdot \mathbf{r}} + \text{c.c.}), \quad |\mathbf{k}_i| = k_c, \quad (3.8)$$

where c.c. denotes the complex conjugate. One-dimensional stripes occur for $m = 1$; two-dimensional stripes may arise for $m = 2$ (rhombic structures) or $m = 3$ with $\mathbf{k}_1 + \mathbf{k}_2 + \mathbf{k}_3 = \mathbf{0}$ (hexagonal structures). Proceeding on to the higher-order inhomogeneous problems, we derive the amplitude equations for the critical modes by formulating the appropriate solvability conditions.

For hexagons we have

$$\begin{aligned} \frac{\partial W_1}{\partial t} = & \kappa W_1 + h_1 W_1 |W_1|^2 \\ & + h_2 W_1 (|W_2|^2 + |W_3|^2) + g W_2^* W_3^*, \end{aligned} \quad (3.9)$$

where

$$\kappa = -\frac{8a_0(y - y_0)}{\Delta^2},$$

$$h_1 = \frac{1}{9} \left[87 + \frac{38\mathcal{C}}{\Delta^2} \right], \quad (3.10a)$$

$$h_2 = 9 \left[1 + \frac{5\mathcal{C}}{9\Delta^2} \right],$$

$$g = -6a_0 \left[1 + \frac{2(y - y_0)}{3\Delta^2 a_0} \left[3 + \frac{2\mathcal{C}}{3\Delta^2} \right] \right]. \quad (3.10b)$$

Similar equations for W_2 and W_3 are obtained from (3.9) by permuting the indices. By setting $W_2 = W_3 = 0$ in Eq. (3.9), we get the amplitude equation for the striped patterns:

$$\frac{\partial W_1}{\partial t} = \kappa W_1 + h_1 W_1 |W_1|^2. \quad (3.11)$$

For rhomboids we have

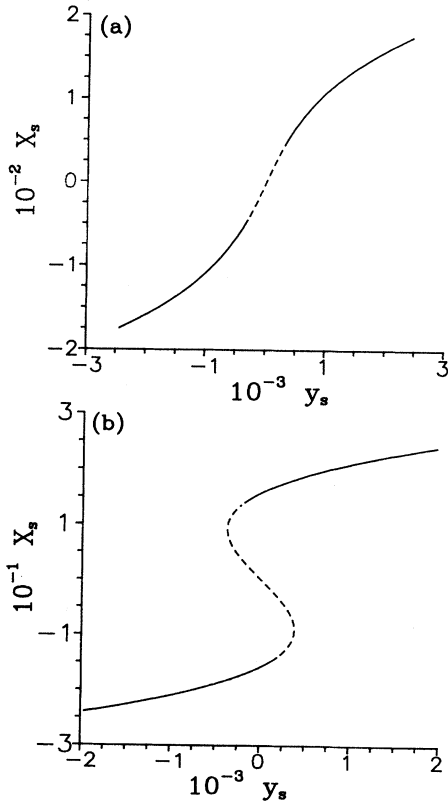


FIG. 1. The homogeneous steady-state curve X_s as a function of y_s , for (a) $\Delta = 0.1, \mathcal{C} = -0.025$ and (b) $\Delta = 0.1, \mathcal{C} = 0.025$.

$$\frac{\partial W_1}{\partial t} = \kappa W_1 + r_1 W_1 |W_1|^2 + r_2 W_1 |W_2|^2 \quad (3.12)$$

with

$$r_1 = h_1, \quad (3.13)$$

$$r_2(\mathcal{C}, \Delta) = \frac{2}{\Delta^2} \left[3\Delta^2 + 2\mathcal{C} + 4(3\Delta^2 + \mathcal{C}) \frac{4 \cos^2 \alpha + 1}{4 \cos^2 \alpha - 1} \right],$$

where α is the angle that \mathbf{k}_1 and \mathbf{k}_2 form on the transverse plane. This last equation holds as long as we stay away from the vicinity of $\alpha \neq 2\pi/3$, in which case the superposition of the two original vectors also lies on the critical circle $|\mathbf{k}_1| = k_c$. The dynamics then of the three interacting modes leads to Eq. (3.9) and the formation of hexagons.

IV. STABILITY OF THE PATTERNS

A discussion of the steady states of the amplitude equations is greatly facilitated if we introduce the polar decompositions $W_i = A_i e^{i\phi_i}$ ($i=1,2,3$). Moreover, we start our analysis with the simplest of the patterns, namely, the stripes.

The equation for the real amplitude A_1 reads as

$$\frac{\partial A_1}{\partial t} = \kappa A_1 + h_1 A_1^3. \quad (4.1)$$

For now we restrict our analysis in the vicinity of the lower bifurcation point of Fig. 1(a) and thus $a_0 < 0$. Equation (4.1) admits two stationary solutions, the trivial one $A_1 = 0$, and $A_{1,s} = \sqrt{\kappa/(-h_1)}$. A linear stability analysis shows that if $h_1 < 0$, the trivial solution remains stable for $y < y_0$, while the nontrivial one bifurcates supercritically and is stable for $y > y_0$. On the other hand, if $h_1 > 0$, the bifurcation is subcritical and thus the emerging solution is unstable. Another bifurcation analysis is then required in order to capture the fifth order saturating nonlinearity. Note, that our bifurcation analysis gives information on stable steady states exclusively in the monostable regime, since the condition $h_1 < 0$ together with (3.3) restricts the range of values of \mathcal{C} to $-3\Delta^2 < \mathcal{C} < -87\Delta^2/38$. The bifurcation structures referred to in the rest of the paper, correspond to $\Delta = 0.1$ and $\mathcal{C} = -0.025$.

In search for patterns with hexagonal symmetry, we employ a similar approach, and in addition we introduce a variable ψ which is the sum of the phases $\psi = \phi_1 + \phi_2 + \phi_3$ and satisfies the equation

$$\frac{\partial \psi}{\partial t} = -g \frac{A_1^2 A_2^2 + A_1^2 A_3^2 + A_2^2 A_3^2}{A_1 A_2 A_3} \sin \psi. \quad (4.2)$$

The equation for the real amplitudes then becomes

$$\frac{\partial A_1}{\partial t} = \kappa A_1 + h_1 A_1^3 + h_2 A_1 (A_2^2 + A_3^2) + g \cos(\psi) A_2 A_3. \quad (4.3)$$

The steady states $\psi_s = 0$ and $\psi_s = \pi$ of Eq. (4.2) give rise to two kinds of hexagonal structures. From now on we refer to them as H0 and H π hexagons, respectively. The domains of their stability are mutually exclusive; the H0's are stable for $g \geq 0$ and the H π 's for $g \leq 0$. As far as the amplitude of the patterns is concerned, we have restricted our search for nontrivial solutions, to symmetric hexagonal structures and found that such a steady state exists and satisfies

$$A_1 = A_2 = A_3 = \frac{-g \cos \psi_s \pm \sqrt{g^2 - 4\kappa(h_1 + 2h_2)}}{2(h_1 + 2h_2)} = A_s. \quad (4.4)$$

The H π ($\psi_s = \pi$) hexagons bifurcate supercritically, but remain unstable in the whole domain of their existence due to the phase instability of Eq. (4.2). On the other hand, the H0 ($\psi_s = 0$) hexagons bifurcate subcritically, this branch corresponds to Eq. (4.4) with the plus sign in front of the square root. A linear stability analysis of the other branch, shows that it is stable with respect to internal amplitude perturbations as long as the following two conditions are simultaneously satisfied:

$$\begin{aligned} \kappa + 3h_1 A_s^2 - g A_s &< 0, \\ \kappa + (3h_1 + 6h_2) A_s^2 + 2g A_s &< 0. \end{aligned} \quad (4.5)$$

The stable branch of H0 hexagons meets the unstable one at the value of y for which $g^2 - 4\kappa(h_1 + 2h_2) = 0$. Below this value both solutions cease to exist.

Finally, rhombic structures can be identified from Eq. (3.12) which in terms of the real amplitudes reduces to

$$\frac{\partial A_1}{\partial t} = \kappa A_1 + r_1 A_1^3 + r_2 A_1 A_2^2. \quad (4.6)$$

The only possible nontrivial symmetric solution is

$$A_1 = A_2 = \sqrt{-\kappa/(r_1 + r_2)}, \quad (4.7)$$

which exists if $r_1 + r_2 < 0$, and is stable if $r_1 - r_2 < 0$. It turns out that these two conditions are mutually exclusive for the range parameters that the bifurcation analysis remains valid, and thus rhomboids are not observed in this model.

We point out that an identical bifurcation analysis of similar structures around the upper critical point in Fig. 1(a) ($a_0 > 0$) shows that the same bifurcation scenarios exist as long as we reverse the respective domains of the bifurcation parameter y .

V. PATTERN SELECTION

So far we have tested the stability of the different patterns against internal perturbations of their respective steady-state solutions. The pattern, though, that the system gets attracted to, when more than one solutions are intrinsically stable and we start from random initial conditions, can be established only via a relative stability analysis. In other words, we have to study the stability of one pattern to perturbations favoring another one.

Therefore, we study the stripe-hexagon competition, by

adding to the stripe solution a small perturbation that consists of three stripes separated by $2\pi/3$ angles (i.e., the perturbation possesses a hexagonal symmetry). Thus, we let

$$A_1 = A_s + u, \quad A_2 = v, \quad A_3 = w, \quad (5.1)$$

where $A_s = \sqrt{\kappa/(-h_1)}$ is the amplitude of the stripe, into the amplitude equation (4.3). In addition, we concentrate on the H0 hexagons which are the only hexagonal structures that exhibit a domain of intrinsic stability in the parameter domain we consider. The linearized system becomes

$$\frac{\partial u}{\partial t} = -2\kappa u, \quad (5.2a)$$

$$\frac{\partial v}{\partial t} = \kappa \left[1 - \frac{h_2}{h_1} \right] v + g A_s w, \quad (5.2b)$$

$$\frac{\partial w}{\partial t} = g A_s v + \kappa \left[1 - \frac{h_2}{h_1} \right] w. \quad (5.2c)$$

Therefore, the perturbation will grow only if

$$\left[\kappa \left[1 - \frac{h_2}{h_1} \right] \right]^2 + g^2 \frac{\kappa}{h_1} < 0. \quad (5.3)$$

This condition identifies an interval close to the origin, the size of which depends on the values of the parameters, where hexagons are more stable than stripes.

We have summarized the results of both the intrinsic and the relative linear stability analysis in the bifurcation diagram of Fig. 2. As we increase the control parameter expressed in relative distance from criticality $(y - y_0)/|y_0|$, a large enough perturbation of the zero state before we reach the bifurcation point, will induce a transition to the H0 hexagons. Subsequently, and for the range of values of the bifurcation parameter complementary to the ones defined by Eq. (5.3), the hexagons give

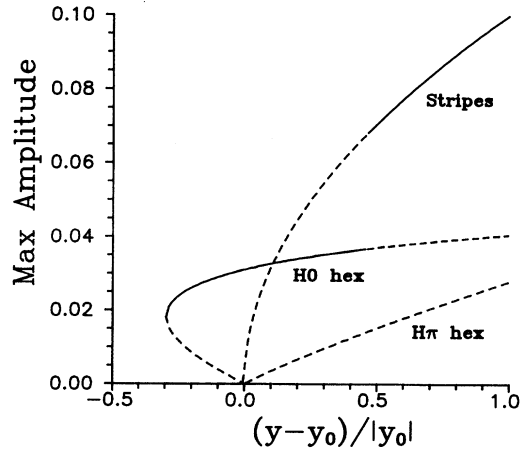


FIG. 2. The complete bifurcation diagram of trivial and non-trivial stationary steady states for the same parameter values as in Fig. 1(a). Solid lines represent stable solutions; dashed lines, unstable ones.

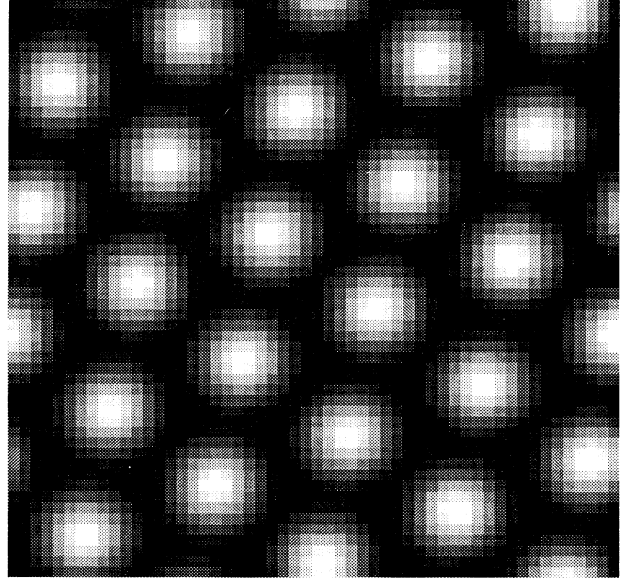


FIG. 3. Stationary hexagonal pattern for $\Delta=0.1$, $\mathcal{C}=-0.025$, and $(y - y_0)/|y_0|=0.3$.

way to stripes. It is evident that a hysteresis arises if we vary the parameter in the opposite direction.

VI. NUMERICAL SIMULATIONS

We have integrated numerically Eq. (2.2) using a pure implicit Euler scheme supplemented by finite difference methods. This scheme reduces the problem to the inversion of a band diagonal matrix. The position of the bands depends on the boundary conditions. We have exclusively looked at periodic boundary conditions. Because of the sparseness of the matrix, we have used the conjugate

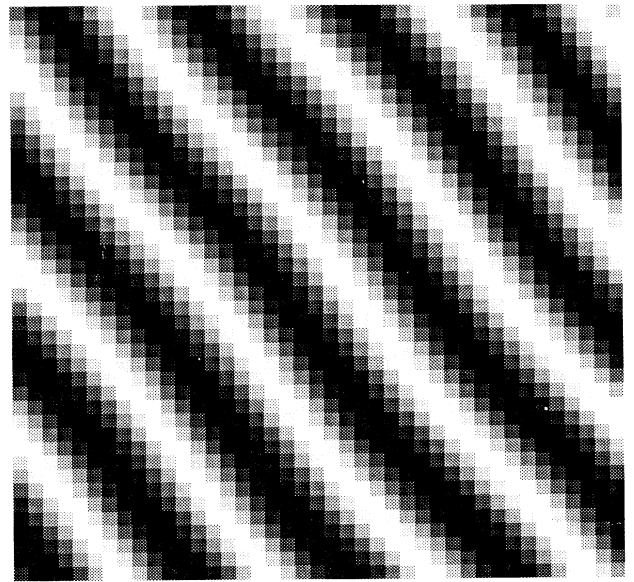


FIG. 4. Stationary striped pattern for $\Delta=0.1$, $\mathcal{C}=-0.025$, and $(y - y_0)/|y_0|=0.7$.

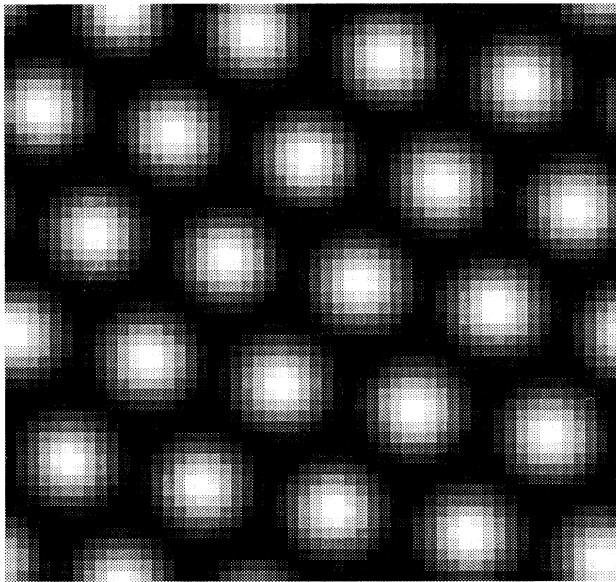


FIG. 5. Hexagonal pattern in the subcritical region, $\Delta=0.1$, $\mathcal{C}=-0.025$, and $(y-y_0)/|y_0|\cong-0.03$.

gradient method. Our simulations are concentrated on the parameter range where the system exhibits monostability to make explicit comparisons with our analytical results. The stationary patterns shown here have been obtained for $\Delta=0.1$ and $\mathcal{C}=-0.025$. For these values of the parameters the linear thresholds are $y_0=\pm 2.7\times 10^{-4}$; we discuss only the lower one. We start our simulations by adding a small amplitude random noise on the homogeneous steady-state solution. As the bifurcation parameter is increased past the threshold, hexagonal structures are observed, the ones shown in Fig. 3 are for $(y-y_0)/|y_0|=0.3$. These hexagons persist up to the value of the bifurcation parameter for which Eq. (5.3) changes sign [here it occurs for $(y-y_0)/|y_0|\cong 0.45$]. In the vicinity of the transition

point, the growth rate of the unstable mode becomes extremely small and therefore long integration times may be required to ensure that the system reaches its asymptotic state. For larger values of the bifurcation parameter, hexagons give way to rolls, the orientation of which depends on the initial conditions. Figure 4 shows rolls for $(y-y_0)/|y_0|=0.7$. In order to capture the hexagons that exist in the subcritical region, we need to impose a large enough perturbation on the system to make sure that it does not return back to the homogeneous state which is also stable below the threshold. The results shown in Fig. 5 for $(y-y_0)/|y_0|=-0.03$, were obtained by starting the simulation above the linear threshold and after reaching the stationary hexagonal pattern moving down the stable hexagonal branch.

VII. CONCLUSION

Our bifurcation analysis on a model of optical bistability reveals the existence of patterns in two transverse dimensions. Unlike the model put forth in [2] by Lugiato and Lefever, the current one allows us to show the transition from hexagonal structures that exist close to the linear threshold, to rolls that persist far away from the threshold. This is unlikely due to the existence of the nonlinear diffusion which is required to balance the growth of the negative linear diffusion term. Our analysis is supported by numerical results, the two methods exhibiting very good agreement.

ACKNOWLEDGMENTS

Stimulating discussions with R. Lefever are gratefully acknowledged. We are indebted to O. Lejeune for his critical help with the numerical simulations. This work has been supported in part by the Fonds National de la Recherche Scientifique, the Interuniversity Attraction Pole programme of the Belgian government, and an EC grant.

-
- [1] N. B. Abraham and W. J. Firth, *J. Opt. Soc. Am. B* **7**, 951 (1990), special issue.
 - [2] L. A. Lugiato and R. Lefever, *Phys. Rev. Lett.* **58**, 2209 (1987).
 - [3] J. V. Moloney and H. M. Gibbs, *Phys. Rev. Lett.* **48**, 1607 (1982).
 - [4] D. W. McLaughlin, J. V. Moloney, and A. C. Newell, *Phys. Rev. Lett.* **54**, 681 (1985).
 - [5] J. V. Moloney, H. Adachihara, R. Indik, C. Lizaragga, R.

- Northcutt, D. W. Laughlin, and A. C. Newell, *J. Opt. Soc. Am. B* **7**, 1039 (1990).
- [6] W. J. Firth, A. J. Scroggie, G. S. McDonald, and L. A. Lugiato, *Phys. Rev. A* **46**, R3609 (1992).
- [7] P. Mandel, M. Georgiou, and T. Erneux, *Phys. Rev. A* **47**, 4277 (1993).
- [8] P. Manneville, *Dissipative Structures and Weak Turbulence* (Academic, New York, 1990).